Chinese Chemical Letters 35 (2024) 109918

Contents lists available at ScienceDirect

Chinese Chemical Letters

journal homepage: www.elsevier.com/locate/cclet

Liquid nitrogen post-treatment for improved aggregation and electrical properties in organic semiconductors

Yuqing Ding[a], Zhiying Yi[a], Zhihui Wang[a,b,*], Hongyu Chen[c,*], Yan Zhao[a,*]

[a] Laboratory of Molecular Materials and Devices, Department of Materials Science, Fudan University, Shanghai 200433, China
[b] Department of Pathology, Changhai Hospital, Naval Medical University, Shanghai 200433, China
[c] Second Medical Center & National Clinical Research Center for Geriatric Diseases, Chinese People's Liberation Army General Hospital, Beijing 100853, China

ARTICLE INFO

Article history:
Received 20 February 2024
Revised 19 April 2024
Accepted 23 April 2024
Available online 24 April 2024

Keywords:
Organic electronics
Environmentally friendly process
Ultralow-temperature post-treatment
Charge carrier mobility
Semiconducting polymer
Organic small molecule

ABSTRACT

Organic semiconductors are promising candidates as active layers in flexible and biocompatible electronics owing to their solution processability and molecular design flexibility. However, it remains necessary to establish a green processing approach to acquire desirable electrical properties for scalable industrial applications. Here, a highly efficient and environmentally friendly post-treatment method using liquid nitrogen as a cooling bath is developed to optimize the aggregation structure and electrical performance of organic semiconductors. The carrier mobility has increased by nearly 60% with this treatment, achieving a performance boost comparable to that of traditional annealing methods. This performance improvement is attributable to the denser aggregation structure and enhanced molecular ordering compared with those of as-cast semiconducting polymer films. Impressively, the entire process can be completed within a few minutes without additional vacuum or high-temperature conditions, offering an economical and efficient alternative to traditional methods. Furthermore, the enhancement effect and long-term stability of this treatment are validated across a wide range of organic semiconductors, positioning this green and versatile approach as a promising substitute for conventional post-treatment, thereby facilitating the development of next-generation sustainable electronics.

In recent decades, organic field-effect transistors (OFETs), which leverage organic semiconductors as active materials, have demonstrated significant potential for application in low-cost, scalable, and flexible electronics, such as displays, biosensors, and wearable electronics [1–3]. The performance of these transistors is intricately linked to the aggregation state of the organic semiconductors [4–6]. Polymeric semiconductors achieve charge transport through jumps within the crystalline regions formed by the ordered stacking of molecular chains, and the transport efficiency is mainly related to the π–π stacking distance [7–10]. Compatible with high-throughput and low-cost OFET solution processing and manufacturing techniques, problems such as imperfect crystallization and disordered molecular chain stacking can occur [11–13]. By subjecting as-cast films to suitable post-treatments, their performance and microstructures can be enhanced [14–16].

Thermal annealing, a crucial post-treatment technique in organic electronics manufacturing, can enhance device performance by providing energy to accelerate polymer chain motion and promote segment rearrangement toward more ordered states [17], thereby tuning the aggregation and morphology [18]. In the domain of organic photovoltaics, annealing can enhance the efficiency of solar cells by refining the crystallinity of the active layer, leading to more effective charge transport and collection [19,20]. For printed electronics, annealing is often used to sinter nanoparticle inks, yielding films with enhanced conductivity [21]. In the case of OFETs [22,23], annealing promotes crystallinity and molecular ordering, thereby boosting charge carrier mobility and resulting in superior electrical characteristics. Overall, in the absence of thermal annealing, the device performance is typically suboptimal.

Solvent vapor annealing is another common treatment method [24–26], which involves exposing a thin film to the vapor of a suitable solvent, resulting in selective swelling and enhanced molecular mobility. This process helps improve the microstructure, *e.g.*, by increasing the size of crystalline domains and enhancing the molecular order, thereby optimizing the performance of electronic and optoelectronic devices [27,28]. For example, Wu *et al.* [29] demonstrated that methyl ethyl ketone steam treatment substantially enhances pentacene OFET performance by reducing the threshold voltage to −0.2 V and achieving a steep subthreshold

* Corresponding authors.
E-mail addresses: zh_wang@fudan.edu.cn (Z. Wang), chenhy0528@163.com (H. Chen), zhaoy@fudan.edu.cn (Y. Zhao).

https://doi.org/10.1016/j.cclet.2024.109918
1001-8417/

slope of 200 mV/dec. These improvements are attributable to the decreased surface state density and reduced deep traps at the pentacene/dielectric interface.

Although these treatment strategies have proven effective, they typically require high-temperature conditions, vacuum environments, or toxic solvents, while treatment process lasts a long period for a few hours or even days, raising serious concerns regarding their environmental sustainability. Therefore, the pursuit of greener and more versatile post-treatment methods with rapid processing cycles to tune the aggregation structure of semiconducting polymers and further to optimize device performance remains paramount. Towards more environmentally friendly objective, this paper develops a novel strategy based on liquid nitrogen cooling (LNC) treatment to effectively enhance the performance of OFETs. Quick cooling of semiconductive thin films *via* immersion in a liquid nitrogen bath, consequently yields films with a shortened stacking distance and enhanced ordered packing morphology compared with those of as-cast films. This optimized aggregation structure significantly improves carrier charge transport with over a 50% increase in mobility, comparable to or exceeding the ratio of thermally annealed devices. Time-stability measurements highlight the establishment of a new equilibrium through LNC treatment in molecular aggregation without relaxation behavior. Notably, the proposed method is highly versatile, proving effective across various organic materials, including n- and p-type polymers and small molecules. In addition to advancing our understanding of organic semiconductor post-treatment, this sustainable approach offers a pathway for large-scale, environmentally friendly fabrication of organic electronic. Considering the effect of temperature on molecular ordering and the requirement of energy conservation, we establish a green post-treatment strategy for optimizing organic semiconductors through a cooling process in liquid nitrogen. We select poly[2,5-bis(2-octyldodecyl)pyrrolo[3,4-*c*]pyrrole-1,4-(2*H*,5*H*)–dione-3,6-diyl-*alt*-(2,2′;5′,2″;5″,2‴-quaterthiophen-5,5‴-diyl)] (DPP-4T3C) as a representative semiconducting material owing to its excellent charge transport ability and investigate the influence of LNC treatment on electrical properties and thin-film morphology.

As shown in Fig. 1, DPP-4T3C is spin-coated onto bottom-contact Au source/drain electrodes patterned on highly doped Si substrates with a SiO_2 dielectric layer modified with octadecyl trichlorosilane (OTS). The obtained OFET device is immediately immersed in a liquid nitrogen bath for ten minutes and then dried in nitrogen. Additionally, an OFET device with the same structure and materials is fabricated and treated with thermal annealing as a reference to evaluate the effect of LNC treatment on the film performance.

To explore the charge transport characteristics pre and post LNC treatment, the OFETs utilizing a bottom-gate/bottom contact (BGBC) device are fabricated. Saturation mobility of OFET devices was determined by analyzing the square root of drain current (I_{DS}) against gate voltage (V_G). Figs. 2a–d depict the transfer and output curves corresponding to these measurements. To accurately quantify and illustrate the performance enhancement after LNC treatment, the corresponding mobilities and changing rates are calculated (Fig. 2e). The transfer characteristics of OFET devices before and after post-treatment processes are measured at room temperature (298 K). The mobility of the LNC-treated BGBC OFET device LNC increases by 60%, from 0.33 $cm^2\ V^{-1}\ s^{-1}$ to 0.53 $cm^2\ V^{-1}\ s^{-1}$. The LNC-treated devices exhibit significantly higher on-current and significantly lower off-current compared with the untreated devices, demonstrating improved charge transfer efficiency. In contrast, the mobility of the thermally annealed device increases only by 45%, from 0.37 $cm^2\ V^{-1}\ s^{-1}$ to 0.54 $cm^2\ V^{-1}\ s^{-1}$. The charge carrier mobility of over thirty OFET devices with DPP-4T3C as active channel was assessed for each treatment method. The average mobility increase with LNC treatment was found to be comparable to that observed with thermal annealing treatment (Fig. S1 in Supporting information). This finding suggests that LNC treatment more notably enhances the carrier charge transport of semiconducting polymers compared with thermal annealing. Under identical experimental conditions, a comparable enhancement effect of LNC treatment is observed in the bottom-gate top-contact (BGTC) device structure, with the charge carrier mobility increasing from 0.38 $cm^2\ V^{-1}\ s^{-1}$ to 0.58 $cm^2\ V^{-1}\ s^{-1}$ (Fig. S2 in Supporting information). Therefore, the effectiveness of the LNC treatment in enhancing charge transport properties is consistent across different device structures, indicating its universal beneficial impact on charge transport properties. Moreover, LNC treatment is less time-intensive and eliminates the need for challenging operating conditions, highlighting its potential as an eco-friendly alternative to the traditional post-treatment method. The current magnitude significantly increases after LNC treatment, as observed in the output curve, which is similar to the treatment effect of annealing.

The improvement in electrical performance is closely linked to changes in the morphology and aggregation structure. Thus, to explore the influence of the cooling process on the morphology of the semiconducting polymer, atomic force microscopy (AFM)

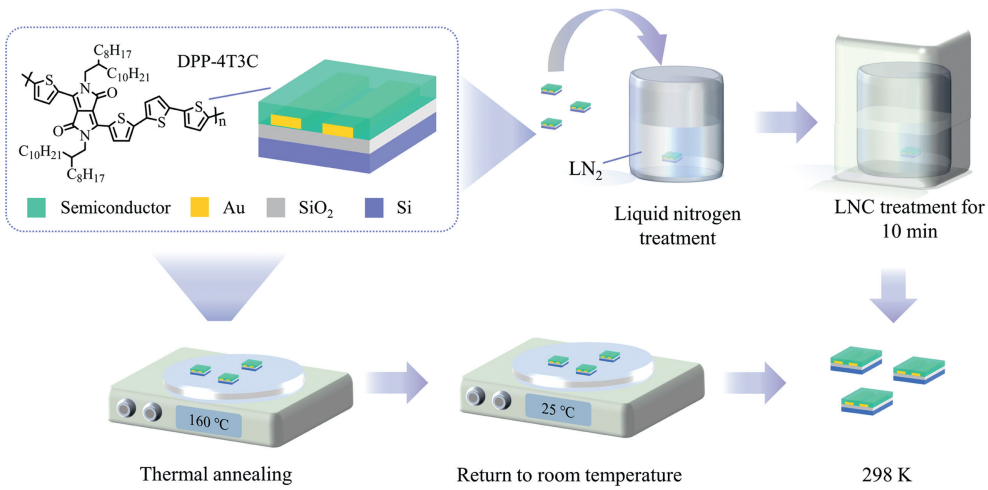

Fig. 1. The molecular structure of the semiconductor used as the active layer, the device structure of OFET, and the schematics of LNC and thermal annealing treatment processes.

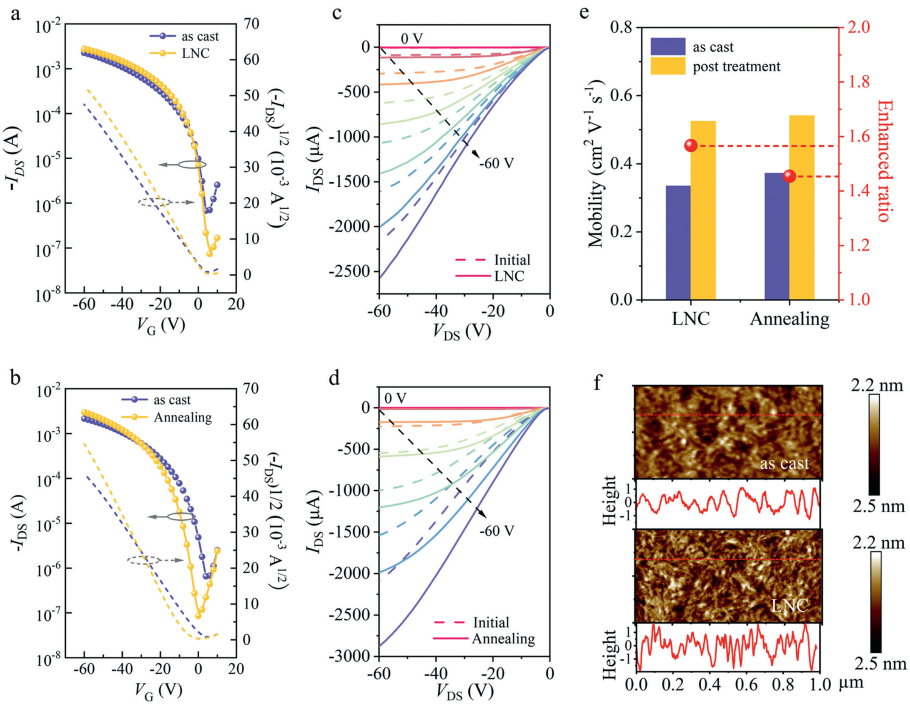

Fig. 2. The electrical performances of the device and surface morphology of the thin films before and after different treatment processes. (a) Typical transfer and (c) output curves of OFETs before and after LNC-treated. (b) Typical transfer and (d) output curves of OFETs before and after thermal annealing. (e) Variation in carrier mobility after different treatment processes. (f) AFM images of the as-cast semiconductor film and LNC-treated film.

measurements are implemented (Fig. 2f). Compared with the surface morphology of the as-cast polymer film, the LNC-treated thin film exhibits reduced grain size and the emergence of a more distinct nanofibrillar structure. Compared with the as-cast polymer film, the surface morphology of LNC-treated film exhibits reduced grain size alongside the emergence of a nanofibrillar structure. Moreover, the root mean square roughness increases from 0.62 nm to 0.76 nm after the treatment, consistent with the trend observed with thermal annealing (Fig. S3 in Supporting information). The surface morphologies of thin films of different organic semiconductors before and after LNC treatment were also characterized, with similar trends observed (Figs. S4 and S5 in Supporting information). The intertwined crystalline structures and interconnected grains contributed to the enhanced device performance [30]. LNC-treated films exhibit a more ordered crystalline structure, which helps minimize charge carrier scattering and obstruction from structural defects [31,32]. Additionally, the X-ray photoelectron spectroscopy (Figs. S6 and S7 in Supporting information) and Raman spectroscopy (Fig. S8 in Supporting information) results show no significant changes, which indicates that LNC treatment does not disrupt the internal structure of the film.

To investigate the changes in aggregation structure and molecular packing pattern induced by the post-treatment process, grazing-incidence X-ray diffraction (GIXRD) measurement are conducted for the as-cast and treated semiconductor films. The schematic diagram of the GIXRD measurement is illustrated in Fig. 3a. As shown in Fig. 3b, both the untreated and LNC-treated films exhibit a typical edge-on orientation. The diffraction pattern and profile lines reveal that LNC-treated films exhibit a stronger peak intensity, indicating the increased crystallinity of the semiconducting polymer. Moreover, Fig. 3c provides 1D-GIXRD line cuts extracted from both the in-plane (Q_{xy}) and out-of-plane (Q_z) directions, offering conclusive evidence of the molecules undergoing a tighter packing arrangement. The detailed crystallographic parameters are summarized in Fig. 3d and Table 1. Notably, the LNC-treated films exhibit a smaller π–π stacking distance (3.63 Å) and

Table 1
Molecular stacking distances and peak FWHM derived from GIXRD analysis of DPP-4T3C.

Post-treatment method	Stacking distance (Å)		FWHM (1/Å)	
	π-π	d-d	π-π	d-d
LNC	3.58	22.86	0.11	0.07
As cast	3.60	22.91	0.11	0.06
Annealing	3.60	22.91	0.11	0.08

lamellar packing distance (23.14 Å) compared with those of the untreated film (3.66 Å and 23.4 Å, respectively). The findings highlight the distinct impact of LNC treatment in decreasing the π-π stacking distance, while the annealing treatment shows negligible influence on the aggregation structure. Furthermore, LNC treatment is applied to films that have undergone annealing, resulting in a reduction in stacking distance to varying degrees (Figs. S9, S10 and Table S1 in Supporting information). This demonstrates the versatility of LNC technology in enhancing the condensed state structure. The closer packing structure can significantly enhance the interchain conjugation interaction, thereby facilitating charge transport among polymer chains, resulting in device performance optimization [33]. The ultraviolet–visible (UV–vis) absorption spectra of the thin films are shown in Fig. S11 (Supporting information). The DPP-4T3C polymer displays distinct double absorption bands in the 200–800 nm range [34], featuring notable 0–1 and 0–0 peaks near 730 nm and 790 nm, respectively. The 0–1 peak corresponds to absorption excited by the disordered aggregated structure, whereas the 0–0 peak indicates absorption excited by the ordered aggregated structure [35,36]. Normalizing the 0–1 peaks to the spectral properties of the polymers reveals significant differences in the absorption characteristics of films before and after LNC treatment. Specifically, LNC-treated films exhibit broader absorption and a slight redshift (~5 nm) of the 0–0 absorption band. This phenomenon suggests an enhanced charge transfer effect in the aggregated state, attributable to tighter π–π stacking in the

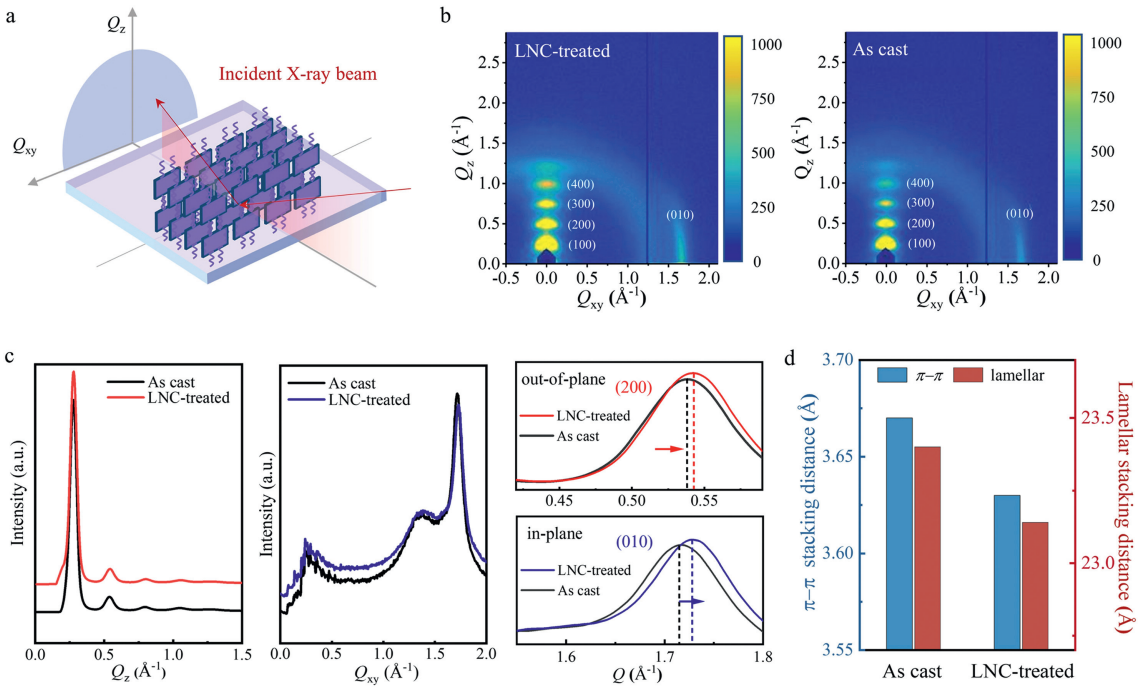

Fig. 3. The experimental setup and results of grazing incidence X-ray diffraction (GIXRD) measurements on semiconductor thin films. (a) Schematic of GIXRD measurement. (b) Diffraction patterns of as cast and LNC-treated semiconductor thin films. (c) 1D-GIXRD line cuts extracted from the in-plane (Q_{xy}) direction and out-of-plane (Q_z) direction. (d) Comparison of stacking distances in out-of-plane and in-plane directions for untreated and treated thin films.

polymer, favoring carrier transport [37–39]. These findings emphasize the role of LNC in the π–π interactions of the polymer chains, consistent with the GIXRD and AFM findings, strongly supporting our claim that the LNC strategy can facilitate the generation of high-crystallinity polymer channel semiconductors for achieving high-performance OFETs at room temperature.

Based on the investigation of the morphology and performance variation of the semiconducting polymer, we identify the mechanism underlying the performance improvement from the perspective of polymer chain motion during LNC treatment [40,41], as depicted in Fig. 4a. In the schematic, L represents the average intermolecular packing distance; ω is the molecular vibration frequency; and V is the free volume of polymer segment, which provides space for molecule motion and is strongly associated with van der Waals' interactions and thermal expansion. Three crucial states appear during LNC treatment, determined by the temperature: (i) At 298 K, pre-treatment. In this state, the molecular chain has an initial free volume of V_1, an average intermolecular packing distance of L_1, and a molecular vibration frequency of ω_1. This state represents the pristine state of the organic semiconductor films prepared at room temperature. (ii) At 77 K, during the cryogenic process. When immersed into liquid nitrogen, the temperature of the semiconductor film instantaneously drops to approach the liquid nitrogen temperature and then stabilizes. (iii) At 298 K, after the treatment. The semiconductor film is extracted from liquid nitrogen, and its temperature gradually recovers to ambient temperature.

In these three states, the semiconductor exhibits distinct thermal motion behaviors and microstructures. In the first state, the aggregation structure is predominantly influenced by the solution preparation process, and it provides the space for molecular motion at room temperature. In the second state, with the instantaneous drop in temperature, the thermal motion of the polymer chains is rapidly weakened as the molecular vibration frequency is significantly reduced to ω_2 ($\omega_2 < \omega_1$). This phenomenon results in the contraction of the free volume ($V_2 < V_1$) and shortened distance between conjugated molecular chains ($L_2 < L_1$). Additionally, the reduced vibration amplitude and shrunk segments contribute to diminished steric resistance, especially among side chains, which promotes the formation of a closer lamellar packing pattern. In the third state, as the temperature rises by 221 K for a brief period, the thermal motion of molecular chains is reactivated as the vibration frequency increases from ω_2 to ω_3 ($\omega_2 < \omega_3$). However, the free volume does not immediately recover to the initial state. The limited space and thermal energy facilitate the elongation and rotation of polymer segments, allowing them to cross the defect barrier and rearrange into a more ordered packing structure. The molecular motion during this process ultimately leads to a smaller free volume (V_3) than that in the initial state, attaining a new equilibrium [42]. Owing to the rearrangement of molecular chains and compression of free volume, the semiconductor films possess more ordered structures and stronger intermolecular interactions between conjugated segments, which enhance both interchain and intrachain charge transport, consistent with the morphology analysis and electrical performance results. The rapid return to room temperature contributes to the maintenance of the aggregated state at low temperatures, which is the key to enhanced charge transport and electrical performance in semiconducting polymer films. Conversely, the slow increase from low temperatures to room temperature does not effectively optimize the aggregation state [4].

The long-term stability of the enhancement effect must be ensured for reliable post-treatment. To exclude the possibility of incomplete thermal relaxation behavior and confirm the establishment of new equilibrium state after low-temperature cooling, we obtain time-dependent measurements of electrical performance characteristics of LNC-treated semiconductor films. Measurements of thermally annealed and untreated thin films are also obtained for comparison. The transfer and output curves are characterized on days 2, 7, 14, 21, and 30 after the treatment process (Fig. 4b). To minimize the interference of environmental factors, all devices are stored in an inert atmosphere.

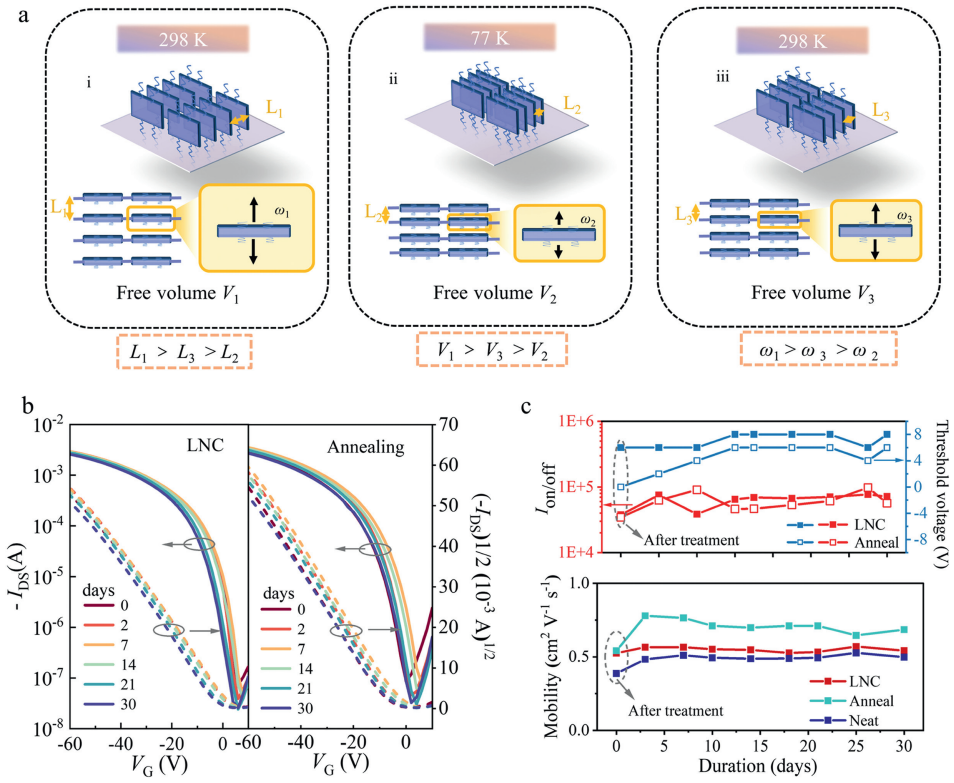

Fig. 4. Mechanism during LNC treatment and the stability measurement. (a) The schematic of the mechanism during LNC treatment, in which L represents the average intermolecular packing distance; ω is the molecular vibration frequency; and V is the free volume of the polymer segment. (b) Shift in transfer curves of LNC-treated and thermally annealed devices over one month. (c) Comparison of changes in mobility, $I_{on/off}$ ratio, and threshold voltage of LNC-treated and thermally annealed devices over 30 days.

The transfer and output characteristics exhibit negligible degradation over one month. As shown in Fig. 4c, all the characteristic parameters exhibit only minor changes over the long-term monitoring period, consistent with the variation trend in the thermal annealing process. It is also observed that the devices treated with LNC consistently demonstrated higher mobility than the untreated ones over a long period (Fig. S12 in Supporting information). This outcome indicates that the treatment-induced variations originate from relative equilibrium formation rather than the relaxation condition. These results demonstrate the reliability and stability of the proposed LNC treatment method in efficiently improving the OFET performance. To investigate the versatility of the proposed LNC treatment method in organic semiconductor systems, it is applied to a diverse array of organic materials, including DPP-based semiconducting polymers (DPPTT and DPPTVT), poly3-hexylthiophene (P3HT), P(NDI2OD-T2) (N2200), and small molecules such as pentacene and C8-BTBT. The molecular structures of these organic semiconductors are depicted in Fig. 5a.

The enhanced ratios of carrier mobilities of the as-cast and LNC-treated semiconductors are summarized in Fig. 5b. LNC treatment considerably enhances the performance ratios, demonstrating its effectiveness in device performance optimization. The performance enhancement is quantified by comparing the carrier mobilities before and after treatment. Fig. 5c and Fig. S13 (Supporting information) present the transfer and output curves of the devices, illustrating the notable improvements in the transfer characteristics of the OFETs post-treatment.

For all tested materials, the mobilities increase after treatment, with the enhancement ratio ranging from 1.3 for pentacene to 2 for DPPTT. The detailed mobilities for each material, both before and after LNC treatment, are outlined in Table S2 (Supporting information). Interestingly, we also discovered that combining thermal treatment with the proposed liquid nitrogen-based treatment can further enhance electrical performance (Fig. S14 and Table S3 in Supporting information). These findings demonstrate that the electrical property enhancement benefits of the post-treatment process are applicable to diverse organic semiconductors, and thus, the proposed approach is well-suited for scalable and environment-friendly applications.

We introduce a novel cost-effective, environment-friendly, and reliable post-treatment technique that can enhance the electrical performance of organic transistors. This method, free from the constraints of strict conditions such as high temperatures and vacuum environments, significantly enhances the carrier mobility of DPP-4T3C from 0.33 cm^2 V^{-1} s^{-1} to 0.53 cm^2 V^{-1} s^{-1}, comparable to the effect of traditional thermal annealing. Morphological analysis reveals a denser aggregation structure and superior molecular ordering in the LNC-treated films, with decreased stacking distances in both in-plane and out-of-plane orientations. This configuration promotes interchain charge transport, contributing to enhanced performance. Additionally, the treatment effects of the proposed approach remain stable over a month, suggesting the induction of a new equilibrium state by the cooling process. Furthermore, the broad applicability of this post-treatment strategy, which can be extended to various organic semiconductor materials including small molecules and polymers, highlights its potential as a universal optimization strategy in the field of organic electronics. These results not only illustrate its potential as a universal optimization strategy but also set the stage for the implementation of sustainable organic electronics in the future.

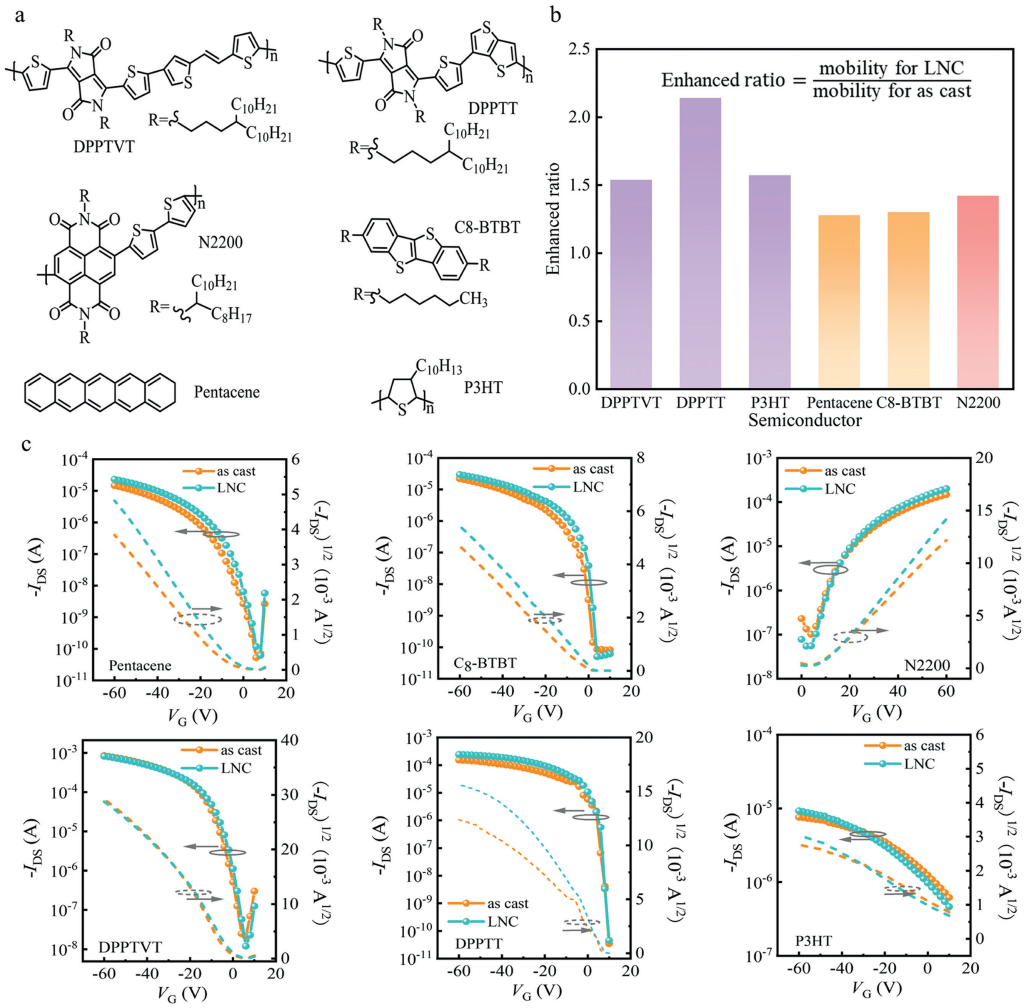

Fig. 5. Versatility of the LNC method in various semiconductor systems. (a) Molecular structures of pentacene, DPP-TVT, DPP-TT, N2200, P3HT, and C8-BTBT. (b) Enhanced ratio after liquid nitrogen treatment (purple column represents p-type polymer, red column represents n-type polymer and orange column represents small molecules) and (c) transfer curves of the six organic semiconductors through as-cast and LNC-treated.

Declaration of competing interest

The authors declare that they have no known competing financial interests or personal relationships that could have appeared to influence the work reported in this paper.

CRediT authorship contribution statement

Yuqing Ding: Writing – review & editing, Investigation. **Zhiying Yi:** Investigation. **Zhihui Wang:** Writing – original draft, Investigation. **Hongyu Chen:** Writing – review & editing, Supervision. **Yan Zhao:** Writing – review & editing, Supervision, Investigation, Conceptualization.

Acknowledgments

This research was supported by the National Key R&D Program of China (No. 2022YFB3603804) and Natural Science Foundation of Shanghai (No. 22ZR1407800).

Supplementary materials

Supplementary material associated with this article can be found, in the online version, at doi:10.1016/j.cclet.2024.109918.

References

[1] H. Chen, W. Zhang, M. Li, et al., Chem. Rev. 120 (2020) 2879–2949.
[2] J. Chen, W. Zhang, L. Wang, G. Yu, Adv. Mater. 35 (2023) 2210772.
[3] Y. Zheng, H. Li, T. Jiang, et al., Chin. Chem. Lett. 35 (2024) 108796.
[4] L. Yang, Y. Wu, Y. Yan, et al., Adv. Funct. Mater. 32 (2022) 2202456.
[5] Q. Chen, Y. Zhao, Y. Liu, Chin. Chem. Lett. 32 (2021) 3705–3717.
[6] W. Huang, Y. Zhang, M. Song, et al., Chin. Chem. Lett. 33 (2022) 2281–2290.
[7] Y. Sun, Y. Guo, Y. Liu, Mater. Sci. Eng. R: Rep. 136 (2019) 13–26.
[8] M. Nikolka, I. Nasrallah, B. Rose, et al., Nat. Mater. 16 (2017) 356–362.
[9] Y. Gao, J. Zhang, D. Liu, et al., Chin. Chem. Lett. 35 (2024) 108582.
[10] A. Mandal, S. Mandal, S.P. Verma, et al., Adv. Mater. Interfaces 10 (2023) 2202293.
[11] Y. Sun, J. Peng, Y. Chen, et al., Sci. Rep. 7 (2017) 46193.
[12] X. Ma, X. Dai, L. Xiang, et al., Chin. Chem. Lett. 35 (2024) 108734.
[13] D.H. Kang, S.Y. Kim, J.W. Lee, N.G. Park, J. Mater. Chem. A 9 (2021) 3441–3450.
[14] T. Wu, X.L. Shi, W.D. Liu, et al., Macromol. Mater. Eng. 307 (2022) 2200411.
[15] K. Chen, N. Xue, G. Liu, et al., Chin. Chem. Lett. 34 (2023) 107884.
[16] Z. Xu, Y. Ni, H. Han, et al., Chin. Chem. Lett. 34 (2023) 107292.
[17] D. Kawaguchi, Polym. J. 55 (2023) 1237–1245.
[18] S. Wang, X. Zhao, C. Zhang, et al., Adv. Mater. 33 (2021) 2101633.
[19] Y. Yang, J. Wang, Y. Zu, et al., Joule 7 (2023) 545–557.
[20] B. Qiu, Z. Chen, S. Qin, et al., Adv. Mater. 32 (2020) 1908373.
[21] J. Liu, J. Garcia, L.M. Leahy, et al., Adv. Funct. Mater. 33 (2023) 2214196.
[22] T. Shen, W. Li, Y. Zhao, et al., Adv. Mater. 35 (2023) 2210093.
[23] Q. Zhou, Z. Wang, Y. Yan, et al., npj Flex. Electron. 7 (2023) 35.
[24] J. Xu, X. Liu, H. Wang, et al., Solid-State Electron. 127 (2017) 61–64.
[25] J. Xu, X. Liu, W. Hou, et al., Bull. Mater. Sci. 41 (2018) 111.
[26] P. Kumar, S. Yadav, N. Kumar, L. Kumar, Solid-State Electron. 176 (2021) 107954.
[27] D. Trefz, Y.M. Gross, C. Dingler, et al., Macromolecules 52 (2019) 43–54.
[28] H. Shan, J. He, B. Zhu, et al., J. Mater. Chem. C 10 (2022) 17583–17593.
[29] J. Wu, H. Zhu, C. Wu, et al., Solid-State Electron. 194 (2022) 108384.

[30] H. Chen, T. Zhao, L. Li, et al., Adv. Mater. 33 (2021) 2102778.
[31] X. Huang, L. Deng, F. Liu, et al., Energy Mater. Adv. 2021 (2021).
[32] K. Janus, D. Chlebosz, A. Janke, et al., Macromolecules 56 (2023) 964–973.
[33] J. Rivnay, M.F. Toney, Y. Zheng, et al., Adv. Mater. 22 (2010) 4359–4363.
[34] Y. Li, P. Sonar, S.P. Singh, et al., J. Am. Chem. Soc. 133 (2011) 2198–2204.
[35] J. Kim, T.M. Swager, Nature 411 (2001) 1030–1034.
[36] M. Li, A.H. Balawi, P.J. Leenaers, et al., Nat. Commun. 10 (2019) 2867.
[37] P.J. Brown, D.S. Thomas, A. Köhler, et al., Phys. Rev. B 67 (2003) 064203.
[38] B.S. Ong, Y. Wu, P. Liu, S. Gardner, Adv. Mater. 17 (2005) 1141–1144.
[39] S.Y. Son, Y. Kim, J. Lee, et al., J. Am. Chem. Soc. 138 (2016) 8096–8103.
[40] E.J. Bailey, K.I. Winey, Prog. Polym. Sci. 105 (2020) 101242.
[41] Z. Wang, Y. Wu, Q. Zhou, et al., Matter 6 (2023) 3434–3448.
[42] R.P. White, J.E.G. Lipson, Macromolecules 49 (2016) 3987–4007.